Evidence for the dissolution of molybdenum during tribocorrosion of CoCrMo hip implants in the presence of serum protein

Thiago A. Simoes[1], Michael G. Bryant[2], Andy P. Brown[1], Steven J. Milne[1], Mary Ryan[3], Anne Neville[2] and Rik Brydson[1]*

[1] Institute for Material Research (IMR), School of Chemical and Process Engineering - SCAPE, University of Leeds, LS2 9JT, UK

[2] Institute of Functional Surfaces (iFS), School of Mechanical Engineering, University of Leeds, LS2 9JT, UK

[3] Department of Materials, Imperial College London, SW7 2AZ, UK

Email:

thiagoasimoes@gmail.com

M.G.Bryant@leeds.ac.uk

A.P.Brown@leeds.ac.uk

S.J.Milne@leeds.ac.uk

m.p.ryan@imperial.ac.uk

A.Neville@leeds.ac.uk

R.M.Drummond-Brydson@leeds.ac.uk

* Corresponding Author: **Prof. Rik Brydson,** Institute for Materials Research**,** School of Chemical and Process Engineering (SCAPE), University of Leeds**,** Leeds LS2 9JT**,** Tel: +113-343 2369**,** Fax: +113-343-2384, e-mail: *R.M.Drummond-Brydson@leeds.ac.uk*

ABSTRACT

We have characterized CoCrMo, Metal-on-Metal (MoM) implant, wear debris particles and their dissolution following cycling in a hip simulator, and have related the results to the tribocorrosion of synthetic wear debris produced by milling CoCrMo powders in solutions representative of environments in the human body. Importantly, we have employed a modified ICP-MS sample preparation procedure to measure the release of ions from CoCrMo alloys during wear simulation in different media; this involved use of nano-porous ultrafilters which allowed complete separation of particles from free ions and complexes in solution. As a result, we present a new perspective on the release of metal ions and formation of metal complexes from CoCrMo implants. The new methodology enables the mass balance of ions relative to complexes and particles during tribocorrosion in hip simulators to be determined. A much higher release of molybdenum ions relative to cobalt and chromium has been measured. The molybdenum dissolution was enhanced by the presence of bovine serum albumin (BSA), possibly due to the formation of metal-protein complexes. Overall, we believe that the results could have significant implications for the analysis and interpretation of metal ion levels in fluids extracted from hip arthroplasty patients; we suggest that metal levels, including molybdenum, be analysed in these fluids using the protocol described here.

KEYWORDS**:** Hip implants; Metal-on-Metal; Wear Debris; Tribocorrosion; ICP-MS.

1. INTRODUCTION

Metal-on-Metal (MoM) hip implants were originally considered a huge advance in prosthetic surgery, particularly for long-term use by younger patients. They have however shown high revision surgery rates which have been linked to material loss, either as implant corrosion or wear [1]. This loss can produce a tissue reaction that may lead to pain, implant loosening and implant failure. In addition, pseudotumors are thought to represent a common adverse reaction to the resulting metal wear debris or dissolved ions, although these have been found in both patients in pain and those with a well-functioning MoM hip implant [2,3].

Biotribocorrosion of these implants, which are typically fabricated from CoCrMo alloys, involves both corrosion of the implant surface itself, which is stimulated by the wear process removing a chromium-rich passivating film, and also mechanical wear of the surface to produce wear debris particles [4,5]; such nanoparticles can be spread by lymphatic circulation and subsequently corrode. Both processes can therefore give rise to the release of metal ions. These may have an inflammatory or toxic effect on cells and tissues, owing to the fact that certain metal ions can complex with proteins and disable their primary function [6–8]. This inflammatory response in turn creates conditions that can accelerate the ion release rate, such as generation of oxidizing species and local acidification.

Current studies on CoCrMo alloy implants confirm that levels of cobalt and chromium ions in the blood/urine rise after replacement surgery and could persist throughout an implant's life; molybdenum levels are not normally monitored because it is considered to be a minor constituent in the alloy [9–11]. As a result there is an ongoing debate concerning the nature and level of the wear debris particles and metal ions released, the transport mechanisms of both the ions and the particles, and the link with inflammation [12]. Whilst the tribocorrosive degradation of orthopaedic devices has been investigated for a number of interfaces [4,13,14], the degradation of the debris produced as a result of wear has been the focus of only a few research studies [15,16].

Wear debris particles generated *in vivo* from CoCrMo implants and found in fixed tissue sections cover a size range of 6 – 834 nm, but are most commonly observed to be around 30 nm in diameter [17–19]. Analysis by transmission electron microscopy (TEM) and energy dispersive X-ray spectroscopy (EDX) of wear debris originally suspended in synovial fluid, extracted from patients with implants reveals three common particulate species: particles with similar composition to the bulk material, particles rich in chromium and molybdenum and also particles composed predominantly of chromium and oxygen [18]; electron energy loss spectroscopy (EELS) in the TEM showed that the majority of these particles were in the Cr(III) oxidation state. Although related to a different interface, involving fretting corrosion at the

taper junction of the stem and femoral head of the implant, Hart *et al.* [20,21] conducted investigations using X-ray Synchrotron radiation (with a 4 µm diameter scanned probe) on tissue sections extracted from regions adjacent to Ultima MoM implants (which exhibit a high failure rate) as well as from non-Ultima MoM implants, both implants being constructed from both high carbon (cup liner and stem) and low carbon (head) CoCrMo ASTM F75 alloys. Here, a chromium phosphate-was shown to be the predominant species in tissue surrounding the non-Ultima implants, whereas analysis of tissue surrounding the Ultima MoM implants revealed a mixture of metallic Co, with a significant amount of Co (II) as the main species, together with some Cr phosphate. The inflammatory response to both metal ions and CoCrMo alloy particles has been highlighted by Caicedo *et al.* [22].

Studies on extracted tissues and fluids surrounding implants are complex to undertake and as a result hip simulators have been developed to mimic the motions and loads experienced by hip implants, so simulating the degradation process and producing both metal ions and wear debris particles. The size of particles produced in artificial hip simulators and tribometers are typically in the range 20-100 nm in diameter [23–25], similar to those produced *in vivo*, but their detailed form could depend on variables such as: the type of simulated body fluid, the number of simulation cycles, the head size and the manufacturer of the implant.

Since hip simulators produce a relatively small amount of wear debris for subsequent testing, it is very difficult to obtain sufficient material for detailed corrosion and toxicological studies of the particles. Hence, recently, an alternative route is to produce larger amounts of synthetic wear debris particles by wet ball milling of powders of the base alloys and then separation of the appropriate size fraction using centrifugal sedimentation [26]. Both hip simulators and ball milling permit studies of the behaviour of particles in different fluid media, enabling investigation of particle dissolution routes during tribocorrosion.

The established technique used to analyse the levels of metal ions in hip simulation fluids is inductively coupled plasma mass spectrometry (ICP-MS), which is conventionally undertaken

following a sample preparation route of centrifugation, extraction of the supernatant, acid digestion and finally ICP-MS analysis. The centrifugation, digestion and dilution procedures are used to reduce clogging of the ICP-MS injector tube, as well as to minimise the influence of any matrix effects which may cause either spectral overlap problems or matrix-induced changes in the intensity of an analyte signal during analysis. Studies of the total mass loss of hip implants due to wear and corrosion have employed this sample preparation route for ICP-MS analysis in order to show that simulated wear debris has a similar composition to that of the bulk alloy [27–29]. Yan *et al.* [30] attempted to separate wear debris particles and ions, produced by pin-on-plate testing in biological solutions, by using centrifugation (10 min, 14000 rpm) prior to ICP-MS analysis. Their results suggested that metal ion contents under open circuit conditions are similar to the bulk alloy composition.

In this study, we demonstrate that centrifugation alone is insufficient to separate nanoparticulate wear debris suspended in simulation media from metal ions dissolved in the same media. Critically we show that a combination of centrifugation and ultrafiltration are required for representative ICP-MS analysis of the products of a number of relevant processes: biotribocorrosion during hip simulation, as well as the tribocorrosion of particles during milling and also their static corrosion during incubation of synthetic wear debris particles. This, more accurate method of separating wear particles and also ions complexed to proteins from dissolved, free ions, allows us to identify a significant, hitherto unexplored, ion release pathway through the body.

2. MATERIALS, METHODS AND METHOD DEVELOPMENT

Hip Simulator Studies

Particulate debris were generated from a 28 mm diameter metal-on-metal hip bearing surface in a Deep Flexion Prosim hip-simulator for 0.3 million cycles (Mc) under ISO loading conditions. A typical twin peak loading cycle, with a peak load of 3 kN and a swing phase of 150 N, was run at a frequency of 1 Hz. Top axis rotation was between +/- 10°, whilst flexion and extension was

between +35° to -15°. The bearing material was wrought CoCrMo high carbon alloy (DePuy). The lubricant used was 12 g/L Foetal Bovine Serum (FBS) plus Phosphate Buffered Saline solution (PBS), supplemented with 0.03% sodium azide to retard bacterial growth (Sigma-Aldrich).

Mechanochemical Milling

This technique will be detailed more fully in a future publication, however it has been shown to produce wear debris with a good approximation of size, shape and composition to that generated *in-vivo* [26,31,32]. It is employed due to the limitations of methods such as hip simulators and pin-on-plate to generate large volumes of CoCrMo nanoparticles in a reasonable amount of time, therefore allowing a more detailed study of the corrosion behaviour of wear debris and its use in subsequent toxicological tests. In addition, milling allows the study of the tribocorrosion of CoCrMo particles in different simulated body environments.

Synthetic wear debris was obtained *via* mechanochemical milling of a micron-sized, gas atomised CoCrMo high carbon powder (Sandvik Osprey – Co212-c) in a SPEX 8000M mill for 150 min, using a ball-to-powder ratio of 3:2, and 40 g/L of Bovine Serum Albumin (BSA) purified by a heat shock process, pH 7.0 (Fisher Scientific), and diluted in MilliQ Water. Milling was also performed in pure PBS solution and Simulated Synovial Fluid (SSF) - a mix of iron-supplemented Calf Serum diluted to a total protein content of 40 g/L with PBS (Sigma-Aldrich). Milling was performed without bacterial control, as samples were also used for subsequent toxicological tests which could potentially affect the results.

Static Corrosion

Following milling of the CoCrMo alloy powders in BSA at pH 7.2, static dissolution studies (incubation) were then conducted over a period of 24 h at 37°C and under both neutral and acid pH conditions, adjusted using HCl (shown at the bottom of Table 1). This latter procedure focused on simulating the different pH environments that metal particles could be exposed to within the human body. The particles were also tested for much longer periods (3, 6, 9 and 12

months) of incubation in BSA, PBS and SSF at 3-4°C, avoiding the temperature range for bacterial growth.

Transmission Electron Microscopy (TEM)

Particulate dispersions at the various stages of sample preparation for ICP-MS were imaged and analysed using a FEI Tecnai F20 field emission (scanning) TEM/STEM operated at 200 kV and fitted with an Oxford Instruments ultrathin window ISIS EDX system. Unless otherwise stated, dispersions were simply drop cast onto holey carbon films supported on TEM grids (Agar Scientific Ltd.). Characterisation of particle morphology was carried out based on the procedure used by Catelas *et al*. [23], who used ratios of the maximum dimensions of each particle measured along orthogonal directions. Particles were classified according to the value of the ratio (r) of length to width and gave information on particle shape: spherical if $1 \leq r < 1.2$, faceted if $1.2 \leq r < 2.5$, and elongated if $r \geq 2.5$. Statistical significance of the results was calculated by ANOVA with a 95% degree of confidence.

Fourier transform infrared spectroscopy (FTIR)

Infrared characterization centrifuged and ultrafiltered supernatants was carried out using a Thermo Scientific Nicolet iS10 FTIR spectrometer running OMNIC processing software, and fitted with an attenuated total reflection (ATR) accessory. Water was used as a background.

Inductively Coupled Plasma Mass Spectrometry (ICP-MS)

Metallic ions present in solution after biotribocorrosion of both CoCrMo hip implants (i.e. hip simulation) and gas atomised microparticles (i.e. milling) were analysed using a Perkin Elmer, Elan DRCe, ICP-MS. The levels of isotopes ^{59}Co, ^{52}Cr and ^{96}Mo were measured.

2.1 Method Development

Recent evidence indicates nanoparticles are ineffectively removed from a supernatant by centrifugation alone [33], hence we employed an alternative route to separate nanoparticles

from ions during ICP-MS sample preparation. Initially three different methods were explored to separate particles and ions in the hip simulator lubricant: firstly, centrifugation at 14,000 rpm for 5-30 min; secondly ultracentrifugation using 40,000-60,000 rpm (a relative Centrifugal Field of 66,700-150,000 x*g*) for 30-60 min; and finally, centrifugation at 14,000 rpm for 10 min, extraction of the supernatant and then further centrifugation at 14,500 rpm (14000 x*g*) for 30 min using a Vivacon® ultrafiltration spin column equipped with a Hydrosart cellulose membrane of 2 kDa molecular weight cut-off (MWCO), corresponding approximately to a pore size of 1.5 nm. The supernatants of the ultracentrifuged samples were analysed by (S)TEM/EDX before acid digestion, as well as the supernatant following centrifugation and ultrafiltration. To prepare TEM samples of these supernatants, grids were simply immersed for 24h in the corresponding liquid, collected and then dried (as per the procedure detailed by Xu *et al*. [33]).

Following each separation process applied to the hip simulator lubricant, 1 ml of each sample was digested in 1 ml of 5% nitric acid for 30 min in an ultrasonic bath (65ºC). The samples were then centrifuged again at 14,000 rpm for 10 min and 0.5 ml of the supernatant was collected and diluted in 8 ml of MilliQ water. Finally, the levels of isotopes ^{59}Co, ^{52}Cr and ^{96}Mo were measured by ICP-MS. For the case of the mechanochemically milled samples, these were diluted 20x and only the centrifugation plus ultrafiltration protocol was used prior to ICP-MS analysis (Table 1).

Following the most severe conditions employed for centrifugal sedimentation of the hip simulator lubricant, i.e. after ultracentrifugation at 60,000 rpm for 60 min, (S)TEM/EDX revealed that the supernatant still contained nanoparticles (Figure 1). For this case, 75 particles in the supernatant were analysed and a preponderance (~55%) of salt particles was found. These had presumably precipitated from the PBS itself during drying (possibly NaCl, KCl, Na_2HPO_4 or KH_2PO_4). Less than 5% of the particles were found to be relatively large and rich in Cr, O and P together with evidence of a thick amorphous coating (see Figure 1A), whereas roughly 40% of particles were observed to be very small Co particles, with only traces of Cr and Mo and these were again suspended in an amorphous or gel-like coating (Figure 1B) containing

N, most likely from the bovine serum albumin. Importantly, samples which had undergone centrifugation followed by ultrafiltration showed an absence of any kind of particles on the TEM grid, indicating that the common procedure of solely using a centrifugation step does not remove all nanoparticles in a supernatant suspension. In order to achieve a good separation of particles and dissolved ions, a physical barrier such as the ultrafilters is required.

The retaining properties of the ultrafilters were assessed using Co, Cr and Mo ionic standards at a concentration of ca. 100 µg/L for each element (purchased from Reagecon). The assays were all performed in triplicate using the following conditions: (a) mix all three standards and dilute in MilliQ water; (b) mix all three standards, dilute in MilliQ water and centrifuge (30 min) using a 2 kDa ultrafilter; (c) mix all three standards, dilute in BSA (40 g/mL) in PBS and centrifuge using a 2 kDa ultrafilter. The corresponding ICP-MS data from the filtrates are shown in Figure 2. The results show no significant difference in the Co, Cr and Mo ionic levels measured in MilliQ water with or without the use of ultrafiltration. Even when Co and Cr ions were placed in BSA+PBS solution, the amounts measured were within the standard deviation of the original concentration. However, Mo shows a significant drop in ionic concentration after exposure to BSA+PBS and ultrafiltration, where only 32% of the Mo ions were recovered. This strongly suggests that the Mo ions could be complexing with the proteins present in BSA[6,34]. The pore size of the ultrafilter is designed to remove proteins larger than 2 kDa as well as removing particles bigger than 1.5 nm, leaving only free metal ions in the filtered solution.

3. RESULTS

3.1 Tribocorrosion during Hip Simulation

Following wear testing in the hip simulator, approximately 100 wear debris particles suspended in the lubricant (without any centrifugation) were analysed by (S)TEM, and particle size, shape and composition were recorded. Particles were found to have an average size of 18 ± 12 nm, with 76 % of particles being faceted, 19 % elongated and 6 % spherical. The majority of the larger particles were found to be Cr-rich and associated with P and O (an example is shown in

Figure 3A). The smaller particles were often more acicular, generally enriched in Co and Mo (see **Figure 3**B) and associated with the presence of N, O and S.

For the hip simulator lubricant samples submitted to just centrifugation or ultracentrifugation, the elemental ratios determined by ICP-MS were found to be broadly comparable to the bulk alloy composition (Co-60, Cr-29%, Mo-7%), but with Mo and Co levels raised by a few percent and Cr levels lowered by similar percentage (Figure 4). The metallic particles already identified in the supernatants by TEM (**Figure 1** - A and B) could easily have been dissolved by the digestion process, or measured directly during ICP-MS. Using ultracentrifugation, the absolute levels of dissolved metal ions are reduced, especially at higher centrifuge speeds and longer times, however the relative elemental ratios remain identical within experimental variation. The use of an ultrafiltration step decreases the absolute level of metal ions by about 6 times, as compared to centrifugation alone, and by about 2 times when compared to ultracentrifugation alone. Importantly though, there is a significant change in the relative elemental ratios (from the base alloy composition) following ultrafiltration, suggesting much higher fractions of Mo (and to a lesser extent Co) dissolution together with release of a very low fraction of Cr during the walking cycle simulation. This marked difference is due to the 2 kDa ultrafiltration step removing nanoparticles and protein complexes prior to ICP-MS analysis, so providing a more representative and accurate level of actual Co and Cr metal ion dissolution, as well as an indication (from figure 2) of both the free Mo ion fraction in solution (about 1/3) and that inferred to be complexed to BSA in solution (about 2/3).

3.2 Tribocorrosion of CoCrMo particles during milling

Mechanochemical milling was also used to compare the release of ions from CoCrMo alloy powders suspended in different media: PBS, BSA and SSF (i.e. salts and serum) under both dynamic milling (tribocorrosion) and static conditions (incubation). Subsequent centrifugation plus ultrafiltration and ICP-MS analysis of CoCrMo alloy particles under dynamic conditions showed that particles milled in PBS released Co and Mo ions in a ratio of about 5:1 (Table 1),

which represents a decrease in Co/Mo ratio as compared to the CoCrMo standard alloy (ca. 10:1). Whilst for material milled in BSA and SSF (both of which contain the same concentration of serum proteins), total Mo levels have to be estimated from that measured in solution and that inferred to be complexed with proteins. Mo is then the dominant ion released in BSA and is in a 1:1 ratio with Co in SSF (Table 1).

3.3 Corrosion of CoCrMo particles as a function of time and environment

Static dissolution studies (incubation) conducted over a period of 24 h under both neutral and acidic pH conditions showed significant solubility of Mo at pH 7.2 and significant Co and Cr solubility only at low pH. Incubation under neutral pH in BSA, reveals Mo as the main element released from the alloy. Cr showed the lowest level of dissolution relative to Co and Mo in all the solutions tested during tribocorrosion. Cr solubility however was clearly enhanced at low pH (4.8), leading to relative levels of ionic release of Co, Cr and Mo that were comparable with the bulk CoCrMo alloy composition; this was the only situation following centrifugation plus ultrafiltration where this behaviour was observed.

The exposure of milled particles for prolonged times in BSA (**Figure 5**) showed Mo as the preferential corrosion species, when taking into account the fact that the level of Mo measured after ultrafiltration is roughly 32% of the total (i.e. accounting for the 68% of Mo ions that interact with BSA and are retained by the ultrafilter, Figure 2). In PBS (**Figure 6**) and SSF (**Figure 7**) Co corrodes from the particles. In terms of the absolute amount of ionic product released, the salt-rich solutions of PBS and SSF released at least twice as many ions as BSA. Cr showed no significant corrosion in all three solutions tested. Serum however appears to play an inverse role in cobalt dissolution; extended exposure times greatly enhanced the release of Mo in the presence of BSA alone, while inhibiting Co release (i.e. potentially acting as a protective bio layer[35]).

3.4 Binding of metal ions to proteins

FTIR spectroscopy of pure BSA and CoCrMo milled in BSA followed by centrifugal sedimentation was carried out with and without ultrafilters. **Figure 8**A displays the FTIR spectrum for BSA diluted in MilliQ water following centrifugation, which indicated the presence of primary and secondary amides [36]. The same absorbances were seen in the FTIR spectrum of CoCrMo particles milled in BSA following centrifugation with an increase in absorption, possibly due to protein coverage on the particle surface (**Figure 8**B). The FTIR spectrum of the solution after CoCrMo particles milled in BSA had been centrifuged and ultrafiltered with a 100 kDa ultrafilter, which removed most of the nanoparticles present in solution is shown in **Figure 8**C. Presumably, the nanoparticles interact with the amide groups in the BSA and, with the removal of these particles *via* ultrafiltration, the signal related to amide groups was correspondingly absent; the solution that remained exhibited absorbances due to C $\equiv$ O and C = O, as well as peaks tentatively assigned to metal carbonyls, which could have formed with the remaining ions in solution [37]. However, this feature could also have been due to the degradation of the proteins in the BSA, post-milling; the proteins in BSA being formed from more than 500 amino acids. Finally, **Figure 8**D shows the FTIR spectrum of the solution after CoCrMo particles milled in BSA had been centrifuged and ultrafiltered with a 30 kDa ultrafilter, which removed up to 95% of the proteins in solution (bovine serum albumin is a 66 kDa protein [38]); here no significant signal was detected in the FTIR spectrum indicting any protein complexes are successfully retained by ultrafilters of 30 kDa and smaller.

4. DISCUSSION

The size of wear debris particles produced by the hip simulator used here, were within the range reported for other hip simulators and also the size of wear debris generated *in vivo* [17,18,39]. After hip simulation, particles were mainly found to be faceted or oval (for 59% of those measured) and composed of Co and Mo (for 39% of those measured), whereas in the hip simulator studies of Catelas *et al*. [23], particles were oval or needle shaped. The studies of Goode *et al.* [17] from explanted tissues reported that the majority of the particles were spherical, however most of the debris had corroded and was more diffuse in nature than the as-worn particles, and some 'needle-like' particles were also observed. The wear debris particle

composition determined by Catelas *et al*. [23] after hip simulation indicated that debris from the 1.75–2 Mc test period (steady-state wear) showed proportionally more chromium oxide particles and fewer needle-shaped particles (mainly CoCrMo) as compared with those from the 0.25 Mc test period (run-in wear). The size and composition of the particles, however, can vary according to the number of simulator cycles, indicating a time-sensitive dissolution process.

Hesketh *et al*. [25] studied metal ion formation during 1 Mc hip simulator tests in Foetal bovine serum diluted in PBS (18 g/L). The cumulative ionic release was determined by ICP-MS at 1/3, 2/3 and 1 Mc. ICP-MS samples were mixed with an equal volume of 5% nitric acid, centrifuged at 14,000 rpm for 10 min and then the supernatant was collected and filtered through a 0.4 μm filter. At 1/3 and 2/3 Mc, the ratio of Cr, Co and Mo ions was fairly constant throughout the test: 29%, 59–60%, and 11–12%, respectively. At 1 Mc, there was more variation, Cr, Co and Mo abundances varied between 16–26%, 60–72% and 11–14%, respectively. These values are close to the relative composition of the base Cr, Co and Mo alloy as might be expected if wear debris particles remain suspended in the supernatant analysed by ICP-MS.

Our revised ICP-MS preparation method has allowed the identification of the dissolution of specific metal elements in different biological media and pH environments (Figure 4 and Table 1). This has revealed dissolution and, by additional assessment of ionic standards in the same media (Figure 2), potential protein complexing of Mo at levels greater than would be expected for the base alloy composition (Figures 5, 6, 7 and 8). The implication of these results is that, unless ultrafiltration is employed, ICP-MS analyses both the underlying ion levels in solution arising as a result of dissolution and protein complexing, plus the alloy wear debris nanoparticles themselves (Figures 1 and 2). Particles rich in chromium and oxygen that were found (Figure 3a) were presumably wear debris CoCrMo particles that have undergone Co and Mo dissolution. Potentially, a complete mass balance of particles, complexes and ions could be achieved in any media by use of a range of MWCO ultrafilters, combined with spectroscopic techniques sensitive to proteins as well as ICP-MS. Such an approach would also require analysis of the appropriate ionic standards in the same media.

Overall, the results show that Cr dissolution from CoCrMo alloys was minimal in biological media under neutral pH, but more pronounced at low pH, such as that which might be found in a lysosome, as discussed by Gill *et al.* [40], it should be noted however that the addition of 0.03% sodium azide during hip simulation may produce more oxidizing conditions increasing the 'baseline' of dissolution at all pHs. A Pourbaix diagram for Cr in water at 25 °C suggests toxic chromium VI is released only at high electrode potentials, and the species generated under acidic conditions is Cr^{3+}, which has a much lower correlation with toxicological issues [40–42]. This agrees with Finley *et al*. [43] who showed that only Cr^{3+} is present in the blood of hip implant patients. Co dissolution appeared to be more significant, particularly in the presence of salt-rich solutions (e.g. PBS and SSF) and at low pH; here the dominant species should be Co^{2+} as is frequently discussed in recent MoM hip implant literature [21,41]. Mechanical attrition of the alloy surface could disrupt the Cr rich passivation layer, which in a protein environment could retard Cr autopassivation properties [44] and expose the Co-rich surface to salts and proteins, drastically increasing the Co ion content in solution [45].

Importantly, significant dissolution of Mo was identified in the presence of serum proteins and at neutral pH. The level of Mo ions in solution following biotribocorrosion in the presence of solutions containing serum proteins (both BSA and SSF) presented here is in agreement with the electrochemical corrosion studies of Espallargas *et al*. [46]. It has been reported that molybdenum ions are essential to the formation of an organic film on the surface of hip implants, which can act as a barrier against electrochemical attack [47,48]. We have shown that the Mo release is most significant into media containing serum proteins at neutral pH. We estimate that this may result in the release of up to 1% of the total Mo from particulate wear debris during static incubation in BSA (the stock concentrations of milled CoCrMo powder prior to incubation was measured to be 20 mg/mL [31] thus containing a total of 1.4 mg/mL Mo and, after incubation, Mo levels were measured by ICP-MS to be 700 μg/L in x20 diluted samples, Figure 5). We expect the dissolved Mo to form a monomeric molybdate anion at neutral pH (MoO_4^{2-}containing Mo^{6+}) and this species is known to complex with the serum proteins present

in the media [6,32,34]. A relatively strong electrostatic interaction could be formed at pH 7 between molybdate anions and positive guanidinium groups in arginine residues in BSA, as has been reported in Arora *et al*. [49] manuscript, and in simulated synovial fluid this would occur in competition with phosphate binding to the same sites. In comparison we would expect Co^{2+} and Cr^{3+} to bind to different sites on BSA as well as the potential for these metals to form phosphates and precipitate at neutral and higher pH.

The observed levels of Co and Cr ions measured in hip implant patients may be the result of the low pH environment surrounding wear debris that has been taken up by phagocytic cells and digested in lysosomes [40]. In addition, metal containing particles could be picked up during serum, synovial fluid or blood collection from patients, thereby confounding mass spectrometry analysis if the sample preparation did not follow a robust protocol for the separation of suspended (nano)particles from ions. Most importantly, Mo levels in these fluids are not commonly assessed and in the light of our data we suggest that they should be measured.

Hallab *et al*. [6] showed that metal ions released by the degradation of CoCrMo particles (ca. 70 µm) could complex with high molecular weight (ca. 180 kDa) proteins. The complexes formed were not identified, however they were shown to be immunologically reactive and capable of inducing lymphocyte activation through proliferation responses. Our current FTIR results show that, following the removal of nanoparticles > 10 nm (i.e. the majority of particles as measured by TEM) via the use of ultrafiltration, absorption peaks related to amides were no longer detected, suggesting protein attachment to the CoCrMo nanoparticles. Another interesting result from FTIR was the appearance of different absorption peaks following removal of the nanoparticles from the solution. There was a change in signal intensity following ultrafiltration, so that any absorption peaks in the region 2200-1900 cm^{-1} that could have been present before filtration, may have been masked due to the strong signal from BSA. These weak peaks could have been related to BSA protein degradation [50] during milling. The amino acids present in BSA solution can provide multiple binding sites for metal free ions. These binding sites may include –NH, –SH, –COOH, and –OH groups, which could have given rise to the absorption peaks

identified. The hypothesis for the formation of metal carbonyl species is initially thought to be unlikely because their synthesis often requires reduction at high temperature and pressure [51]. However, Hart *et al*. [20] detected similar molybdenum species in tissue from MoM hip patients using X-ray Absorption Near and Extended Edge Structure (XANES and EXAFS). This study indicated an octahedrally coordinated molybdenum species bound by oxygen and then carbon in the second coordination sphere. In addition, Dolamic and Burgi (2011) have shown that the degradation of amino acids such as L-asparagine and L-glutamic acid, both present in BSA, can give rise to new complexes with metallic species [52]. The importance of identifying the possible existence of metal carbonyl species as a result of wear from hip implants is related to the high toxicity of these species [53,54] and specifically, the impact of Mo on the formation of these and similar complexes must now be considered. This is particularly relevant to higher Mo content alloys, such as those used in implant stems.

In summary, our studies have explored the importance of the correct measurement of metallic ions in solution during the tribocorrosion of hip implants. Using our new procedure we have clarified the influence of nanoparticles on dissolution studies and hence revealed relatively high levels of molybdenum-containing ions that could be complexed with proteins. In general terms, the role of metal ions in biological processes is widely discussed in literature [55,56], in addition there are many recent reports about the toxicity of nanoparticles which quickly dissolve, releasing toxic ions [57–59]. Although there is not a great deal of literature on molybdenum, Scharf *et al.* [60] have reported Co and Cr metal ions binding to proteins and inducing loss of their biological function. Yang and Black [55] have shown that free metal ions, such as cobalt, could saturate at concentrations of around 2 moles per 1 mole of albumin serum. *In-vivo* these metal ions could be surrounded by an overabundance of serum as healthy joints can contain between 15-25 g/L of protein concentration (17 g/L is recommendation of ISO standard 14243 for simulations). However, it is known that diseased or inflamed joints with diseases could present even higher protein concentrations, in the range of 36– 54 g/L [61].

From the pre-clinical point of view, the benefit of this new analytical method is that it allows an effective discrimination between the three wear products produced during tribocorrosion: free (metal) ions, complexed (metal) ions and (metal) nanoparticles (where the metal in the latter is nominally in a zero valence state). This allows us to determine exactly where metallic ions are originating from during tribocorrosion processes and then allows a direct correlation of corrosion measurements with ICP-MS data; highlighting any additional ions that may come from the dissolution of nanoparticle wear debris. In this respect, we suggest that there are possible shortfalls in the ASTM/ ISO standards related to the ICP-MS procedure for ionic concentration measurements in these systems which need to be addressed.

5. CONCLUSIONS

In this work we have highlighted that the commonly reported techniques of separating nanoscale wear debris from lubricant fluids using only centrifugation or ultracentifugation are sub-optimal and lead to residual wear nanoparticles suspended in the analyte fluid. This can cause a large overestimation of the absolute and relative amounts of ionic dissolution that occur during the tribochemical wear of CoCrMo alloy samples. This has significant implications for the analysis of serum, synovial fluid and blood samples from patients exhibiting an adverse reaction to prosthetic hip surgery.

The use of a centrifugation plus ultrafiltration step during ICP-MS sample preparation can efficiently remove nanoparticulate wear debris and metal-protein complexes that remain in the supernatant after centrifugal sedimentation. This revised preparation method has allowed the identification of the dissolution of specific metal elements in different biological media and pH environments. These have revealed the dissolution of Mo in the presence of serum proteins, and that, based on the pH dependence, it is likely that more significant Co and Cr solubility will only occur if particles are taken up by phagocytic cells and digested in lysosomes. Specifically, in the case of salt rich solutions, Co dissolution is enhanced. In addition, FTIR showed that a fraction of the dissolved metal ions, in majority Mo ions, could be forming complexes as a result of the dissociation of the amino acids found in BSA, possibly driven by the energy input from

either, the milling process or any mechanical contact at the implant surface, if the conditions are severe enough. Finally, there may be implications for use of higher Mo content alloys in implants, and we suggest that Mo ion levels in relevant fluids should be monitored, in addition to the more usual analysis of Co and Cr levels.

FUNDING SOURCES

This work was supported by the CAPES - Brazilian Federal Agency for Support and Evaluation of Graduate Education within the Ministry of Education of Brazil [grant numbers BEX-5515/10-6].

ACKNOWLEDGMENT

We thank Andrew Beadling for hip simulator samples and Dr AE Goode and Dr AE Porter for valuable discussions. Guidance on metal-protein complexes was also provided by Prof. Anne Duhme-Klair at York University as well as Dr Claudia Blindauer at Warwick University and of the BBSRC Metals in Biology Network.

ABBREVIATIONS

MoM, Metal-on-Metal; ICP-MS, Inductively Coupled Plasma Mass Spectrometry; BSA, Bovine Serum Albumin; TEM, Transmission Electron Microscopy; EDX, Energy Dispersive X-Ray Spectroscopy; EELS, Electron Energy Loss Spectroscopy; Mc, million cycles; FBS, Foetal Bovine Serum; PBS, Phosphate Buffered Saline; FTIR, Fourier transform infrared spectroscopy; SSF, Simulated Synovial Fluid; MWCO, Molecular Weight Cut-Off.

REFERENCES

[1] NJR, National Joint Registry for England and Wales 9th Annual Report, 2012. www.njrcentre.org.uk.

[2] A.K. Matthies, J.A. Skinner, H. Osmani, J. Henckel, A.J. Hart, Pseudotumors are common in well-positioned low-wearing metal-on-metal hips, Clin. Orthop. Relat. Res. 470 (2012) 1895–906.

[3] A.K. Matthies, R. Racasan, P. Bills, L. Blunt, S. Cro, A. Panagiotidou, G. Blunn, J. Skinner,

A.J. Hart, Material loss at the taper junction of retrieved large head metal-on-metal total hip replacements, J. Orthop. Res. 31 (2013) 1677-85.

[4] Y. Yan, A. Neville, D. Dowson, S. Williams, Tribocorrosion in implants-assessing high carbon and low carbon Co-Cr-Mo alloys by in situ electrochemical measurements, Tribol. Int. 39 (2006) 1509–1517.

[5] P. Ponthiaux, R. Bayon, F. Wenger, J.-P. Celis, Testing protocol for the study of bio-tribocorrosion, in: Bio-Tribocorrosion Biomater. Med. Implant., Elsevier, 2013: pp. 372–394.

[6] N.J. Hallab, K. Mikecz, C. Vermes, A. Skipor, J.J. Jacobs, Orthopaedic implant related metal toxicity in terms of human lymphocyte reactivity to metal-protein complexes produced from cobalt-base and titanium-base implant alloy degradation, Mol. Cell. Biochem. 222 (2001) 127–36.

[7] I. Catelas, A. Petit, D.J. Zukor, J. Antoniou, O.L. Huk, TNF-alpha secretion and macrophage mortality induced by cobalt and chromium ions in vitro - Qualitative analysis of apoptosis, Biomaterials. 24 (2003) 383–391.

[8] K. Magone, D. Luckenbill, T. Goswami, Metal ions as inflammatory initiators of osteolysis, Arch. Orthop. Trauma Surg. 135 (2015) 683–695.

[9] A. Massè, M. Bosetti, C. Buratti, O. Visentin, D. Bergadano, M. Cannas, Ion release and chromosomal damage from total hip prostheses with metal-on-metal articulation, J. Biomed. Mater. Res. B. Appl. Biomater. 67 (2003) 750–7.

[10] J.H. Dumbleton, M.T. Manley, Metal-on-Metal Total Hip Replacement, J. Arthroplasty. 20 (2005) 174–188.

[11] M.C. Rizzetti, P. Liberini, G. Zarattini, S. Catalani, U. Pazzaglia, P. Apostoli, A. Padovani, Loss of sight and sound. Could it be the hip?, Lancet. 373 (2009) 1052.

[12] D. Cohen, How safe are metal-on-metal hip implants?, Br. Med. J. 344 (2012) e1410–e1410.

[13] J. Hesketh, Q. Meng, D. Dowson, A. Neville, Biotribocorrosion of metal-on-metal hip replacements: How surface degradation can influence metal ion formation, Tribol. Int. 65 (2013) 128–137.

[14] B. Alemón, M. Flores, W. Ramírez, J.C. Huegel, E. Broitman, Tribocorrosion behavior and ions release of CoCrMo alloy coated with a TiAlVCN/CNx multilayer in simulated body fluid plus bovine serum albumin, Tribol. Int. 81 (2015) 159–168.

[15] F. Billi, P. Benya, E. Ebramzadeh, P. Campbell, F. Chan, H.A. McKellop, Metal wear particles: What we know, what we do not know, and why., SAS J. 3 (2009) 133–42.

[16] Y. Yan, A. Neville, D. Dowson, S. Williams, J. Fisher, Effect of metallic nanoparticles on the biotribocorrosion behaviour of Metal-on-Metal hip prostheses, Wear. 267 (2009) 683–688.

[17] A.E. Goode, J.M. Perkins, A. Sandison, C. Karunakaran, H. Cheng, D. Wall, J.A. Skinner, A.J. Hart, A. E. Porter, D. W. McComb, M.P. Ryan, Chemical speciation of nanoparticles surrounding metal-on-metal hips, Chem. Commun. (Camb). 48 (2012) 8335–7.

[18] M.B. Ward, A.P. Brown, A. Cox, A. Curry, J. Denton, Microscopical analysis of synovial fluid wear debris from failing CoCr hip prostheses, J. Phys. Conf. Ser. 241 (2010) 12022.

[19] P.F. Doorn, P.A. Campbell, J. Worrall, P.D. Benya, H.A. McKellop, H.C. Amstutz, Metal wear particle characterization from metal on metal total hip replacements: transmission electron microscopy study of periprosthetic tissues and isolated particles, J. Biomed. Mater. Res. 42 (1998) 103–11.

[20] A.J. Hart, P.D. Quinn, B. Sampson, A. Sandison, K.D. Atkinson, J.A. Skinner, J. Powell, J.F.W Mosselmans, The chemical form of metallic debris in tissues surrounding metal-on-metal hips with unexplained failure, Acta Biomater. 6 (2010) 4439–4446.

[21] A.J. Hart, P.D. Quinn, F. Lali, B. Sampson, J.A. Skinner, J.J. Powell, et al., Cobalt from metal-on-metal hip replacements may be the clinically relevant active agent responsible for periprosthetic tissue reactions, Acta Biomater. 8 (2012) 3865–3873.

[22] M.S. Caicedo, R. Desai, K. McAllister, A. Reddy, J.J. Jacobs, N.J. Hallab, Soluble and particulate Co-Cr-Mo alloy implant metals activate the inflammasome danger signaling pathway in human macrophages: a novel mechanism for implant debris reactivity., J. Orthop. Res. 27 (2009) 847–54.

[23] I. Catelas, J.D. Bobyn, J.B. Medley, J.J. Krygier, D.J. Zukor, O.L. Huk, Size, shape, and composition of wear particles from metal-metal hip simulator testing: effects of alloy and

number of loading cycles., J. Biomed. Mater. Res. A. 67 (2003) 312–27.

[24] R. Pourzal, I. Catelas, R. Theissmann, C. Kaddick, A. Fischer, Characterization of wear particles generated from CoCrMo alloy under sliding wear conditions, Wear. 271 (2011) 1658–1666.

[25] J.L. Tipper, P.J. Firkins, A.A. Besong, P.S.M. Barbour, J. Nevelos, M.H. Tone, E. Ingham, J. Fisher, Characterisation of wear debris from UHMWPE on zirconia ceramic, metal-on-metal and alumina ceramic-on-ceramic hip prostheses generated in a physiological anatomical hip joint simulator, Wear. 250 (2001) 120–128.

[26] T.A. Simoes, A.E. Goode, A.E. Porter, M.P. Ryan, S.J. Milne, A.P. Brown, R.M.D Brydson, Microstructural characterization of low and high carbon CoCrMo alloy nanoparticles produced by mechanical milling, J. Phys. Conf. Ser. 522 (2014) 12059.

[27] J.P. Kretzer, M. Krachler, J. Reinders, E. Jakubowitz, M. Thomsen, C. Heisel, Determination of Low Wear Rates in Metal-On-Metal Hip Joint Replacements Based on Ultra Trace Element Analysis in Simulator Studies, Tribol. Lett. 37 (2009) 23–29.

[28] C. Heisel, Characterization of the Running-in Period in Total Hip Resurfacing Arthroplasty: An in Vivo and in Vitro Metal Ion Analysis, J. Bone Jt. Surg. 90 (2008) 125.

[29] I. Leslie, S. Williams, C. Brown, G. Isaac, Z. Jin, E. Ingham, J. Fisher, Effect of bearing size on the long-term wear, wear debris, and ion levels of large diameter metal-on-metal hip replacements-An in vitro study., J. Biomed. Mater. Res. B. Appl. Biomater. 87 (2008) 163–72.

[30] Y. Yan, D. Dowson, A. Neville, In-situ electrochemical study of interaction of tribology and corrosion in artificial hip prosthesis simulators., J. Mech. Behav. Biomed. Mater. 18 (2013) 191–9.

[31] T.A. Simoes, A.P. Brown, S.J. Milne, R.M.D. Brydson, CoCrMo nanoparticles produced by mechanochemical milling: a route to simulate wear debris from hip implants, in: XIII Brazilian Mater. Res. Soc. Meet., 2013.

[32] T.A. Simoes, A.P. Brown, S.J. Milne, R.M.D. Brydson, Bovine Serum Albumin binding to CoCrMo nanoparticles and the influence on dissolution, J. Phys. Conf. Ser. 644 (2015) 12039.

[33] M. Xu, J. Li, N. Hanagata, H. Su, H. Chen, D. Fujita, Challenge to assess the toxic contribution of metal cation released from nanomaterials for nanotoxicology-the case of ZnO nanoparticles, Nanoscale. 5 (2013) 4763–9.

[34] W.R. Hagen, Cellular uptake of molybdenum and tungsten, Coord. Chem. Rev. 255 (2011) 1117–1128.

[35] M.T. Mathew, C. Nagelli, R. Pourzal, A. Fischer, M.P. Laurent, J.J. Jacobs, M.A. Wimmer, Tribolayer formation in a metal-on-metal (MoM) hip joint: An electrochemical investigation, J. Mech. Behav. Biomed. Mater. 29 (2014) 199–212.

[36] P. Huang, Z. Li, H. Hu, D. Cui, Synthesis and Characterization of Bovine Serum Albumin-Conjugated Copper Sulfide Nanocomposites, J. Nanomater. 2010 (2010) 1–6.

[37] S.K. Samvelyan, V.T. Aleksanyan, B.V. Lokshin, Band intensities in the infrared spectra of metal carbonyl complexes: Chromium, molybdenum and tungsten hexacarbonyls, J. Mol. Spectrosc. 48 (1973) 47–56.

[38] S. Guedes, R. Vitorino, R. Domingues, F. Amado, P. Domingues, Oxidation of bovine serum albumin: identification of oxidation products and structural modifications., Rapid Commun. Mass Spectrom. 23 (2009) 2307–15.

[39] I. Catelas, J.B. Medley, P. a Campbell, O.L. Huk, J.D. Bobyn, Comparison of in vitro with in vivo characteristics of wear particles from metal-metal hip implants., J. Biomed. Mater. Res. B. Appl. Biomater. 70 (2004) 167–78.

[40] H.S. Gill, G. Grammatopoulos, S. Adshead, E. Tsialogiannis, E. Tsiridis, Molecular and immune toxicity of CoCr nanoparticles in MoM hip arthroplasty., Trends Mol. Med. 18 (2012) 145–55.

[41] M.G. Shettlemore, K.J. Bundy, Examination of in vivo influences on bioluminescent microbial assessment of corrosion product toxicity., Biomaterials. 22 (2001) 2215–28.

[42] J. Guertin, Toxicity and Health Effects of Chromium (All Oxidation States), in: Chromium(VI) Handb., CRC Press, 2004: pp. 215–234.

[43] B. Finley, P.K. Scott, M.E. Glynn, D. Paustenbach, E. Donovan, K.A. Thuett, Chromium speciation in the blood of metal-on-metal hip implant patients, Toxicol. Environ. Chem. (2016) 1–17.

[44] J.R. Goldberg, J.L. Gilbert, Electrochemical response of CoCrMo to high-speed fracture of its metal oxide using an electrochemical scratch test method., J. Biomed. Mater. Res. 37 (1997) 421–31.

[45] T. Hanawa, Metal ion release from metal implants, Mater. Sci. Eng. C. 24 (2004) 745–752.

[46] N. Espallargas, C. Torres, A.I. Muñoz, A metal ion release study of CoCrMo exposed to corrosion and tribocorrosion conditions in simulated body fluids, Wear. 332–333 (2014) 669–678.

[47] Y.L. Chou, J.W. Yeh, H.C. Shih, The effect of molybdenum on the corrosion behaviour of the high-entropy alloys Co1.5CrFeNi1.5Ti0.5Mox in aqueous environments, Corros. Sci. 52 (2010) 2571–2581.

[48] E.J. Martin, R. Pourzal, M.T. Mathew, K.R. Shull, Dominant Role of Molybdenum in the Electrochemical Deposition of Biological Macromolecules on Metallic Surfaces, Langmuir. 29 (2013) 4813–4822.

[49] J.P.S. Arora, R.P. Singh, S.S. Jain, S.P. Singh, A. Kumar, 701—The interaction between bovine serum albumin and molybdate ions, Bioelectrochemistry Bioenerg. 13 (1984) 329–342.

[50] J.-M. Brandt, K.D.J. Charron, L. Zhao, S.J. MacDonald, J.B. Medley, Commissioning of a displacement-controlled knee wear simulator and exploration of some issues related to the lubricant., Proc. Inst. Mech. Eng. H. 225 (2011) 736–52.

[51] W. Gresham, J.V.E. Hardy, Synthesis of metal carbonyls, (1949).

[52] I. Dolamic, T. Bürgi, In Situ ATR-IR Study on the Photocatalytic Decomposition of Amino Acids over Au/TiO 2 and TiO 2, J. Phys. Chem. C. 115 (2011) 2228–2234.

[53] R.A. Goyer, T.W. Clarkson, Toxic Effects of Metals, 5th editio, McGraw-Hill, New York, 1996.

[54] M. Ardon, P.D. Hayes, G. Hogarth, Microwave-Assisted Reflux in Organometallic Chemistry: Synthesis and Structural Determination of Molybdenum Carbonyl Complexes. An Intermediate-Level Organometallic-Inorganic Experiment, J. Chem. Educ. 79 (2002) 1249.

[55] J. YANG, J. BLACK, Competitive binding of chromium, cobalt and nickel to serum proteins,

Biomaterials. 15 (1994) 262–268.

[56] Metals in chemical biology, Nat. Chem. Biol. 4 (2008) 143–143.

[57] T.B. Kardos, Cellular responses to metal ions released from implants., J. Oral Implantol. 40 (2014) 294–8.

[58] S. Chen, A.E. Goode, S. Sweeney, I.G. Theodorou, A.J. Thorley, P. Ruenraroengsak, Y. Chang, A. Gow, S. Schwander, J. Skepper, J. Zhang, M. S. Shaffer, K.F. Chung, T. D. Tetley, M.P. Ryan, A.E. Porter, Sulfidation of silver nanowires inside human alveolar epithelial cells: a potential detoxification mechanism, Nanoscale. 5 (2013) 9839.

[59] O.M. Posada, D. Gilmour, R.J. Tate, M.H. Grant, CoCr wear particles generated from CoCr alloy metal-on-metal hip replacements, and cobalt ions stimulate apoptosis and expression of general toxicology-related genes in monocyte-like U937 cells., Toxicol. Appl. Pharmacol. 281 (2014) 125–135.

[60] B. Scharf, C.C. Clement, V. Zolla, G. Perino, B. Yan, S.G. Elci, E. Purdue, S. Goldring, F. Macaluso, N. Cobelli, R.W. Vachet, L. Santambrogio, Molecular analysis of chromium and cobalt-related toxicity, Sci. Rep. 4 (2014) S35-41.

[61] J.-M. Brandt, L.K. Brière, J. Marr, S.J. MacDonald, R.B. Bourne, J.B. Medley, Biochemical comparisons of osteoarthritic human synovial fluid with calf sera used in knee simulator wear testing, J. Biomed. Mater. Res. Part A. 94 (2010) 961–71.

FIGURE LEGENDS

Figure 1. Bright field TEM images and EDX of: (A) Cr and (B) Co nanoparticles found in the supernatant of the hip simulator lubricant following ultracentrifugation at 60000 rpm for 60 min.

Figure 2. ICP-MS of Co, Cr and Mo ionic standards incubated in three conditions: only mixed in milliQ water, mixed in water and passed through an ultrafilter (2 kDa MWCO) and finally mixed with BSA (40g/L)+PBS and passed through an ultrafilter (2 kDa MWCO).

Figure 3. Bright field TEM images of: (A and B) wear particles from the hip simulator lubricant. Key EDX spectra are shown in panel C.

Figure 4. Metal elemental levels in supernatants of hip simulator fluids, measured by ICP-MS after the different sample preparation procedures indicated on the x-axis. Results are given as the average of duplicate assays, with the error bar indicating the standard deviation. The percentage values are given for comparison to the bulk alloy.

Figure 5. Ionic release of CoCrMo milled in BSA particles over time, as measured by ICP-MS following the centrifugation plus ultrafiltration procedure. Mo* is an estimate of the total Mo dissolution (i.e., that measured by ICP-MS after ultrafiltration plus that estimated to be retained by the ultrafilter, Figure 2).

Figure 6. Ionic release of CoCrMo milled in PBS particles over time, as measured by ICP-MS following the centrifugation plus ultrafiltration procedure.

Figure 7. Ionic release of CoCrMo milled in SSF particles over time, as measured by ICP-MS following the centrifugation plus ultrafiltration procedure. Mo* is an estimate of the total Mo

711 dissolution (i.e., that measured by ICP-MS after ultrafiltration plus that estimated to be retained
712 by the ultrafilter, Figure 2).
713
714 **Figure 8.** FTIR spectra of: A. BSA solution showing peaks of Amide I and II; B. CoCrMo milled and
715 centrifuged nanoparticles in BSA solution showing the Amide I and II peaks; C. CoCrMo milled
716 and centrifuged nanoparticles in BSA solution after the use of a 100 kDa MWCO ultrafilter
717 revealing potential metal carbonyl bonds; D. after the use 30 kDa MWCO ultrafilter all strong
718 absorption peaks are eliminated.
719
720 **Table 1.** Metal elemental levels in supernatant samples following centrifugation plus
721 ultrafiltration and ICP-MS of CoCrMo powders milled in different environments. Results are
722 given in both absolute terms (μg/L) and also relative terms (%). Measured Mo values in the
723 presence of serum are indicated by ( )*. Total Mo values are reported assuming only 32% of
724 the total dissolved Mo ions are measured in solution by ICP-MS after ultrafiltration (i.e. when in
725 the presence of serum 68% are estimated to be retained by the ultrafilter, Figure 2).
726

FIGURE 1

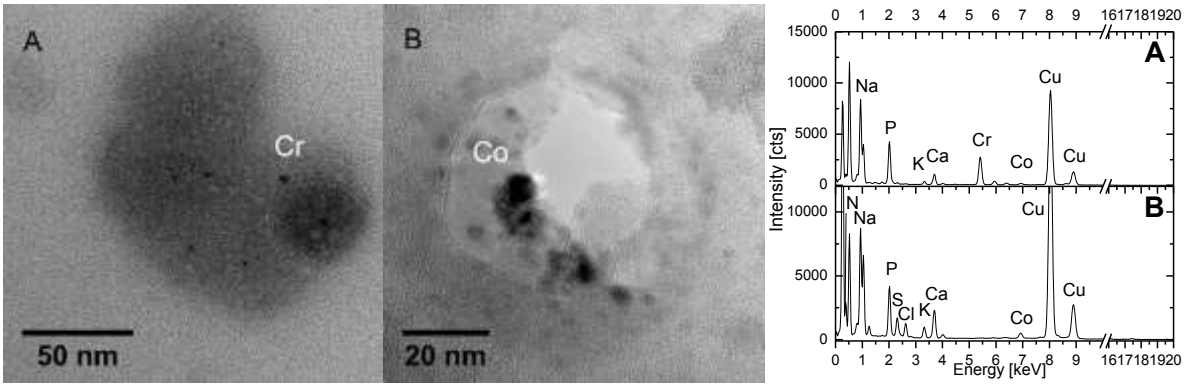
A
Cr
50 nm
B
Co
20 nm
A
B
Na
P
K
Ca
Cr
Co
Cu
N
S
Cl
Intensity [cts]
Energy [keV]

FIGURE 2

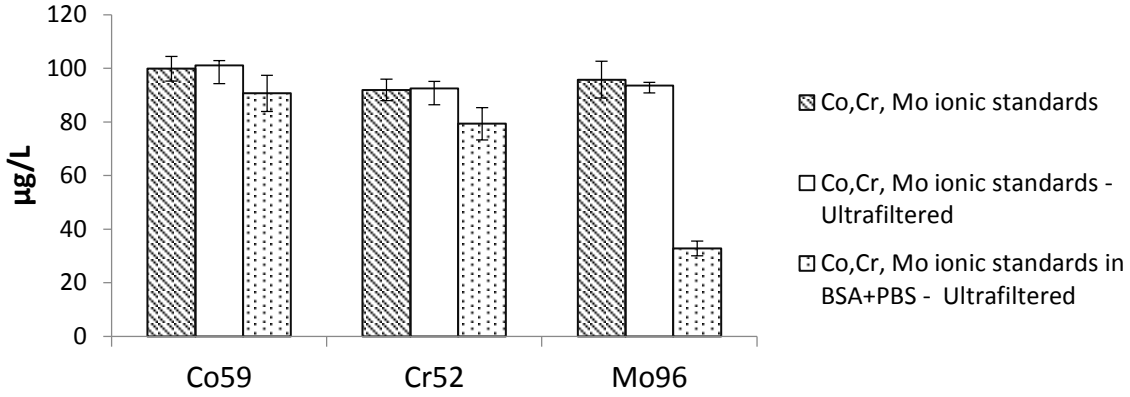
120
100
80
60
40
20
0
µg/L
Co59
Cr52
Mo96
Co,Cr, Mo ionic standards
Co,Cr, Mo ionic standards - Ultrafiltered
Co,Cr, Mo ionic standards in BSA+PBS - Ultrafiltered

FIGURE 3

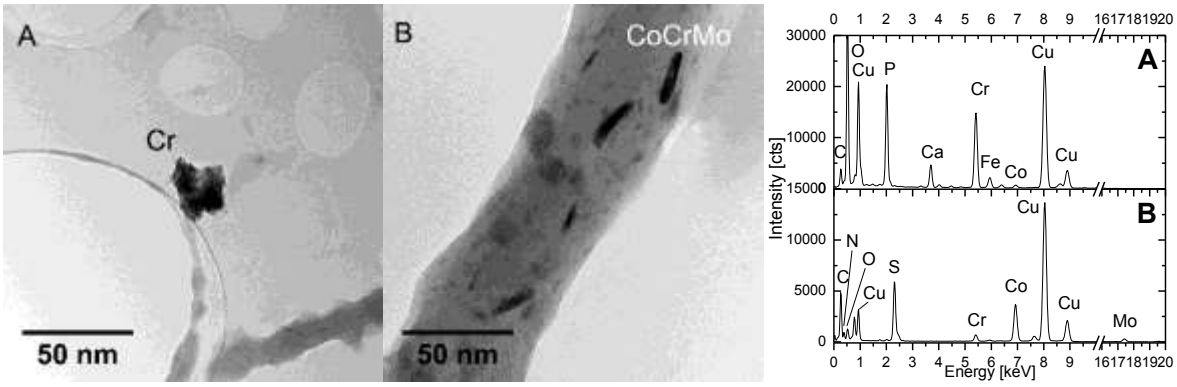
A
Cr
50 nm
B
CoCrMo
50 nm
Intensity [cts]
Energy [keV]
A
O
Cu
P
Cr
Ca
Fe
Co
Cu
C
B
N
O
S
Cu
C
Co
Cu
Cr
Mo

FIGURE 4

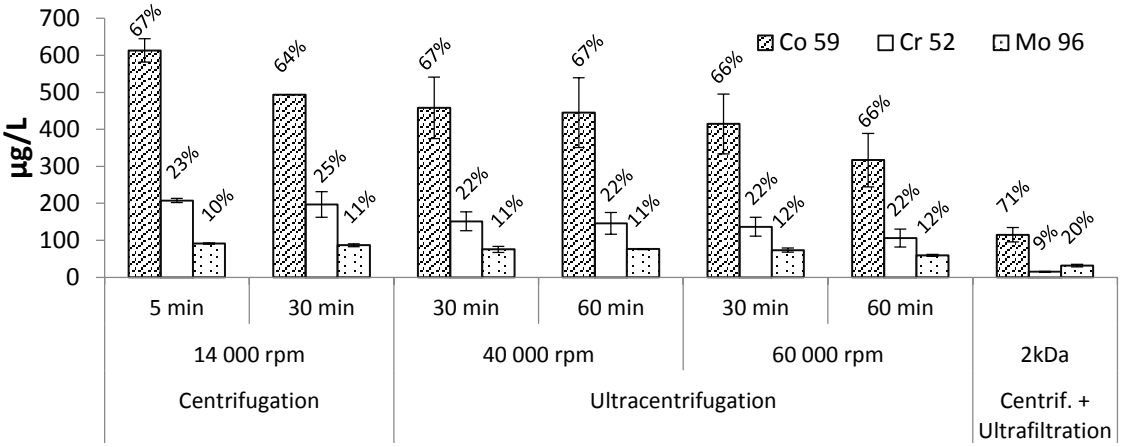
µg/L
700
600
500
400
300
200
100
0
Co 59
Cr 52
Mo 96
67%
23%
10%
64%
25%
11%
67%
22%
11%
67%
22%
11%
66%
22%
12%
66%
22%
12%
71%
9%
20%
5 min
30 min
30 min
60 min
30 min
60 min
14 000 rpm
40 000 rpm
60 000 rpm
2kDa
Centrifugation
Ultracentrifugation
Centrif. +
Ultrafiltration

TABLE 1

		Cobalt [µg/L]	Sdt	[%]	Chromium [µg/L]	Sdt	[%]	Molybdenum [µg/L]	Sdt	[%]
Dynamic Conditions (Milling)	PBS [pH 7.2]	174.4	2.3	82.9%	0.3	0.0	0.2%	35.6	3.9	16.9%
	BSA [pH 7.2]	33.1	5.5	12.1%	0.6	0.0	0.2%	239.8(76.7)*	11.8	87.7%
	SSF [pH 7.2]	157.0	2.6	48.6%	0.8	0.0	0.3%	16.3(52.9)*	4.6	51.2%
Static Conditions (incubated 24h)	BSA [pH 7.2]	0.7	0.1	3.3%	0.2	0.1	1.0%	20.0(6.4)*	0.7	95.7%
	BSA [pH 4.8]	16.4	0.2	565%	4.8	0.2	16.5%	7.8(2.5)*	0.2	26.9%

753 **FIGURE 5**
754

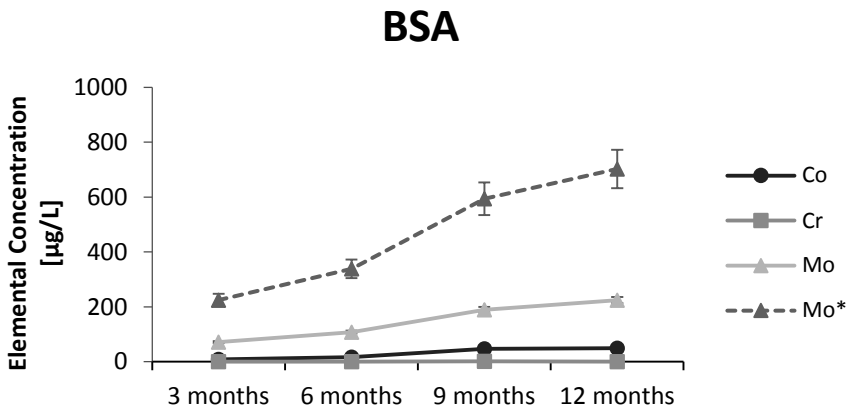

755
756
757

FIGURE 6

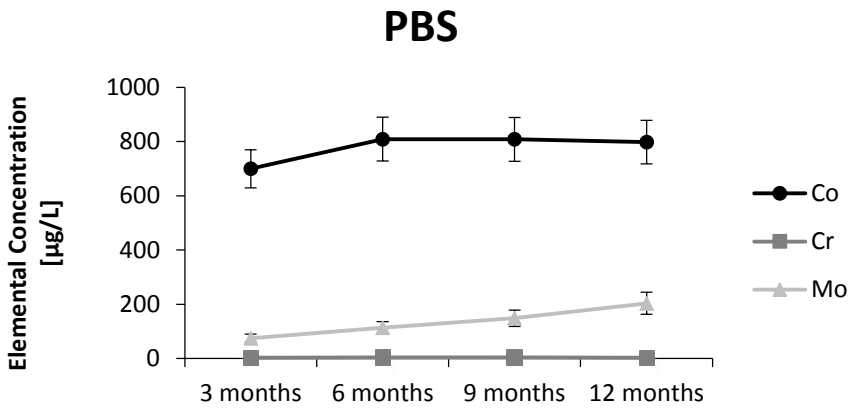
PBS
Elemental Concentration [µg/L]
1000
800
600
400
200
0
3 months
6 months
9 months
12 months
Co
Cr
Mo

FIGURE 7

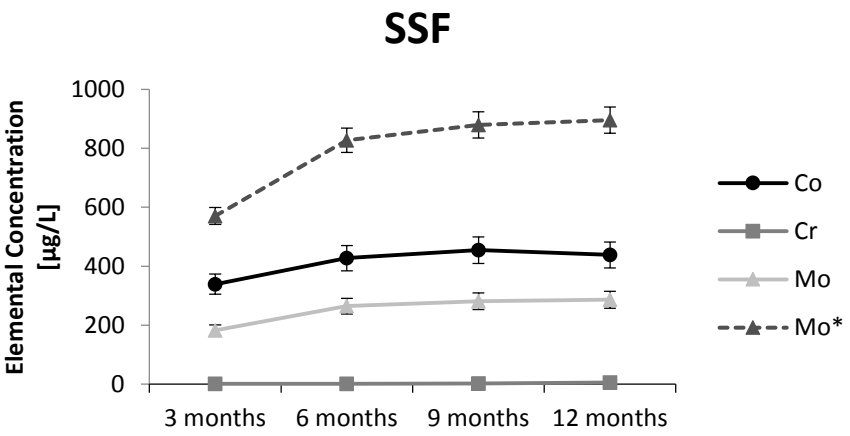
SSF
Elemental Concentration [µg/L]
1000
800
600
400
200
0
3 months
6 months
9 months
12 months
Co
Cr
Mo
Mo*

FIGURE 8

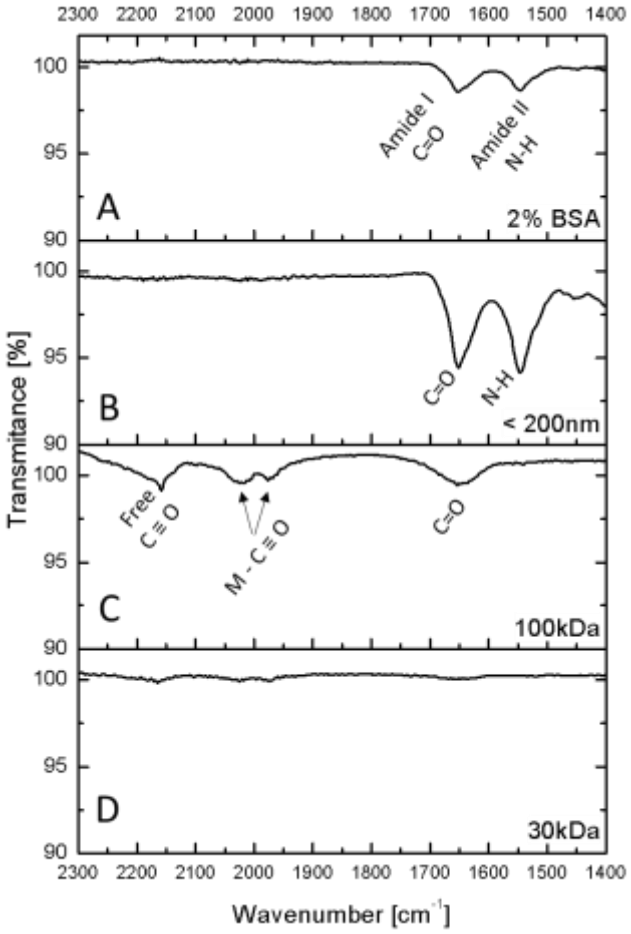
2300 2200 2100 2000 1900 1800 1700 1600 1500 1400
100
95
90
Amide I
C=O
Amide II
N-H
A
2% BSA
B
C=O
N-H
< 200nm
Free
C≡O
M - C≡O
C=O
C
100kDa
D
30kDa
Transmitance [%]
Wavenumber [cm-1]